Asia-Pacific Journal of Science and Technology: Volume: 29. Issue: 06. Article ID.: APST-29-06-13. Research Article

APST

Asia-Pacific Journal of Science and Technology

https://www.tci-thaijo.org/index.php/APST/index

Published by the Research Department,
Khon Kaen University, Thailand

# Optimizing the placement and content of burnable poison in Gama-Float reactor's fuel assembly

Daniel A. Prasetyo, Alexander Agung* and Sihana

Department of Nuclear Engineering and Engineering Physics, Universitas Gadjah Mada, Yogyakarta, Indonesia
*Corresponding author: a_agung@ugm.ac.id

Received 6 September 2023
Revised 21 March 2024
Accepted 27 May 2024

## Abstract

Floating Nuclear Power Plant (FNPP) is used to potentially fulfil the energy needs of a remote region. In this context, a new FNPP reactor named Gama-Float was designed to tackle different issues. The first stage of the design process was producing a fuel assembly design without burnable poison. However, the design was inadequate at beginning-of-cycle (BOC) since multiplication factor ($k_\infty$) was relatively high and required compensation. Therefore, this research aimed to develop an optimization process using the Method of Characteristics for neutronic calculations in achieving a better design based on a genetic algorithm. The results showed that optimization must satisfy two objectives, namely lowering the multiplication factor and maintaining the fuel cycle length. A subsequent analysis was carried out to select results from the optimization. In this context, the assemblies' initial multiplication factor, fuel cycle length, and power peaking factor (PPF) were analyzed and the final design was selected based on the analysis. The initial multiplication factor and fuel cycle were reduced to 1.0054 and 3644.41 days, while the radial PPF increased to 1.2789 at BOC in an acceptable range. These results highlight the effectiveness of the optimization process in improving neutronic performance and fuel cycle efficiency for the Gama-Float reactor.

**Keywords:** Burnable poison, Genetic Algorithm, Method of Characteristics, Optimization

## 1. Introduction

Indonesia as an archipelagic country is subjected to different challenges in fulfilling energy requirements. Generally, this issue is manifested in remote regions where the demand is small and dispersed, with over 300 villages lacking access to electricity [1]. The development of the region posed a significant challenge since the current energy supply relies on precarious fossil fuels such as coal. In this context, the use of Floating Nuclear Power Plant (FNPP) is an option to address the issues. The power plant has several advantages in solving issues, where high mobility and energy density allow the reactor to be deployed in unreachable regions without constant fuel supply.

Currently, one of the FNPPs in operation is KLT-40s and this reactor was designed by JSC "Afrikantov OKB Mechanical Engineering" [2]. KLT-40s is a pressurized Water Reactor (PWR) with 150 MWt thermal power and water coolant. A suitable design is needed to tackle the energy issues in remote regions since the power output of KLT-40s reactor is unsuitable for regions with less demand.

FNPP research team from Universitas Gadjah Mada developed a reactor named Gama-Float to tackle the issue of fulfilling energy requirements [3]. Gama-Float is a Pressurized Water Reactor with rectangular fuel assemblies. The first stage of development to design a fuel assembly with an extended fuel cycle has been conducted. The design is inadequate as the multiplication factor ($k_\infty$) at beginning of cycle (BOC) is relatively high. Meanwhile, large excess reactivity requires a large amount of neutron absorbers (control rods), leading to increased power generation in the region with fewer neutron absorbers, resulting in non-uniform power generation [4]. An increase in power during transient results in a pellet-cladding interaction, compromising the integrity of the fuel pin [5,6].

Other methods to compensate for the excess reactivity include the usage of soluble boron in the coolant. However, this practice does not suit a high multiplication factor because a coolant with a high concentration of

soluble boron can form positive reactivity feedback during a loss of coolant accident (LOCA) [7]. Lowering $k_\infty$ value is also achieved by introducing neutron absorber material in the fuel assembly configuration [8,9].

Burnable poison (BP) as a neutron absorber was selected over soluble boron to simplify the reactor design. In this context, the elimination of soluble boron removes boron-induced reactivity accidents and gains a negative moderator reactivity coefficient [10]. The removal also creates several advantages by removing the corrosive effects of soluble boron [11]. Meanwhile, the absorber selected must conserve the fuel cycle length and lower the $k_\infty$ at BOC. Gadolinium oxide ($Gd_2O_3$) form is burnable poison and the isotopic composition in gadolinium (Gd) improves the evolution of the fuel assembly's multiplication factor [12]. Compared to other BP (such as boron (B), erbium (Er), europium (Eu), samarium (Sm), dysprosium (Dy)), Gd has an extremely fast depletion rate and the residual reactivity is very small. Samarium also depletes very rapidly but has a significant burnup penalty [13,14]. The residual reactivity of the boron is negligible and depletes slowly. For Er, Eu, and Dy, the depletion is relatively slow with a high residual reactivity [13]. $^{157}Gd$ has high absorption cross sections, lowering the parasitic absorption due to enrichment of 70%. The isotope was shown to perform better than natural Gd [15,16]. The calculation of BP in fuel assembly is carried out by implementing a deterministic or stochastic method to an optimization method. Therefore, this research aims to determine the optimal ratio and configuration of Gd for Gama-Float fuel assembly. Burnable poison design should conserve the fuel cycle length with no parasitic absorption toward end-of-cycle (EOC). In addition, the design needs to lower $k_\infty$ at BOC without compromising the result in the cycle.

## 2. Materials and methods

The decision regarding the optimization algorithm and burnable poison selection is based on other results [9,13,14,16-18]. This decision includes using 70% enriched Gd and a genetic algorithm optimization method with the weight factor as the fitness function. The placement of Gd in the fuel assembly follows two arrangements, namely integral fuel burnable absorber (IFBA), as shown in Figure 1(A) and homogeneous burnable poison, as shown in Figure 1(B). For the IFBA arrangement, burnable poison is placed as an outer ring of $Gd_2O_3$ on the fuel pellet inside the cladding. Meanwhile, the other arrangement, the homogeneous burnable poison, and the placement of $Gd_2O_3$ in the fuel form a homogeneous mix. Each arrangement uses a 70% enriched $Gd_2O_3$, with the isotopic composition presented in Table 1.

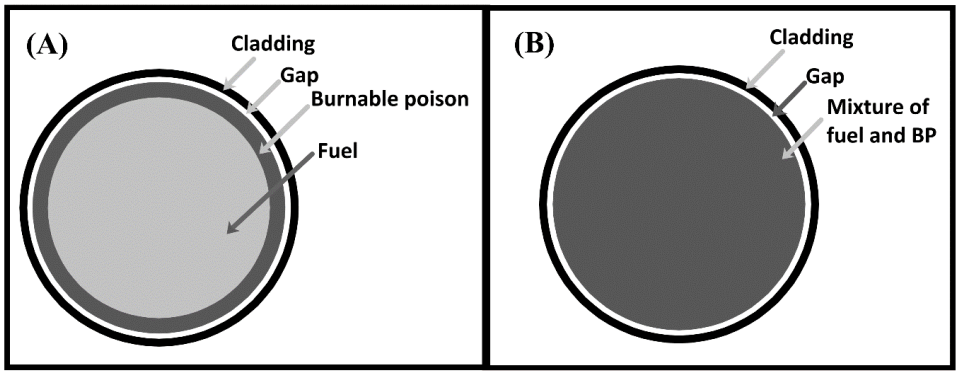


**Figure 1** Model for burnable poison type, in which A is the integral fuel burnable absorber and B is the homogeneous burnable poison.

**Table 1** The isotopic composition of 70% enriched Gd [16].

| Isotope | Percentage (%) |
|---|---|
| Gadolinium-152 | 0.071 |
| Gadolinium-154 | 0.747 |
| Gadolinium-155 | 5.160 |
| Gadolinium-156 | 7.219 |
| Gadolinium-157 | 70.000 |
| Gadolinium-158 | 8.883 |
| Gadolinium-160 | 7.920 |

The modeling process is performed with Polaris, which is a lattice physics module for light water reactor fuel in SCALE 6.2. In this context, Embedded Self-Shielding Method (ESSM) is used for multigroup cross-section processing through Bondarenko interpolation. For the $k_{eff}$ calculation, a new Method of Characteristics transport solver developed by the Exnihilo computational package is used [19]. The model is a 2-D lattice with a quarter symmetry in the southeast region of the fuel assembly. Moreover, the basic configuration follows the previous

research that FNPP team has conducted and presented in Table 2. The assembly configurations will remain the same except for the fuel radius of IFBA poison and material for homogeneous burnable poison pins. Burnup calculation is performed with adjusted timesteps and the selection should be carried out before the optimization. Subsequently, a set of different timesteps is evaluated, and an optimal set is selected. The optimal set of timestep include 0, 1, 2, 4, 8, 30, 120, 240, 360, 480, 960, 1400, 2200, 3000, and 3700 days.

**Table 2** The basic configuration of the fuel assembly [3].

| Pin | Fuel material | Cladding material | P/D | Fuel radius (cm) | Cladding thickness (cm) | Total diameter (cm) | Fuel enrichment (%) |
|---|---|---|---|---|---|---|---|
| 10×10 | $U_3Si_2$ | FeCrAl | 1.34 | 0.4033 | 0.030 | 0.8846 | 7.70 |
| 11×11 | $U_3Si_2$ | FeCrAl | 1.60 | 0.3707 | 0.030 | 0.8194 | 6.79 |
| 12×12 | UN | FeCrAl | 1.81 | 0.3621 | 0.030 | 0.8022 | 7.51 |
| 13×13 | UN | SiC | 1.56 | 0.4100 | 0.057 | 0.9520 | 7.17 |
| 14×14 | $U_3Si_2$ | SiC | 1.41 | 0.5197 | 0.057 | 1.1714 | 6.39 |
| 15×15 | $U_3Si_2$ | SiC | 1.72 | 0.4642 | 0.057 | 1.0604 | 6.53 |
| 16×16 | $U_3Si_2$ | FeCrAl | 1.62 | 0.4543 | 0.030 | 0.9866 | 6.67 |
| 17×17 | $U_3Si_2$ | FeCrAl | 1.46 | 0.4233 | 0.030 | 0.9246 | 6.90 |

Burnup is essential for calculating the fuel cycle length and multiplication factor. The calculation is performed with interpolation based on multiplication factor on the multiple points. The model is performed with the method of characteristics in solving the Boltzmann transport equation while calculating the Bateman equation using the Chebyshev rational approximation method (CRAM) simultaneously. Meanwhile, Method of Characteristics has been successfully applied and implemented in many reactor analysis codes for solving partial differential equations. This is achieved by implementing an algorithm for ray tracing along each characteristic line to compute solutions [20, 21]. CRAM uses a rational function to approximate the exponential matrix solution [22] and the Bateman equation needs to be written in terms of coefficients in a matrix [23].

Based on the calculation from burnup, two parameters are derived for the optimization, namely fuel cycle length and change in multiplication factor at BOC. These two parameters are used to construct the fitness for each fuel assembly configuration. Considering the dual objectives within the optimization problem, a function that amalgamates the two objectives into a singular fitness value is important. The simplest method includes formulating a calculation where each objective is assigned a weight and aggregated to generate a cumulative sum [24]. However, an appropriate weight is needed to ensure the conduction of the optimization. In this context, Equation (1) presented a function to derive the fitness. The weight fractions are skewed in favor of the initial weight and the fractions are distributed as 0.55-0.75 for the first and 0.45-0.25 for the second. Following normalization, the weight factors (w1 and w2) adopt values in the range of 0.55-0.75 and 4500-2500, respectively. To determine the optimal weight factor, five variations are selected for the analysis as presented in Table 3. For w1, and w2 the corresponding objective is the fuel cycle length and change in the initial multiplication factor, respectively. The difference in the order of magnitude requires a different method of formulating the weight. In addition, the weights are supposed to be fractions with a cumulative sum. The differences in the objective's numerical value ($10^3$ and $10^{-1}$) required adjusting the weights. Therefore, the second weight is normalized by multiplying with a multiplication factor of $10^4$. The normalization gave the fitness components the same numerical value of $10^3$, which balances the formulation of the function. Each variation is used to formulate the fitness function for the genetic algorithm and a sample of 20 individuals is taken from the result. An analysis is performed to comprehend the relationship between fitness and objectives after the appropriate weight is found. Meanwhile, the optimization is performed using the genetic algorithm according to the flowchart shown in Figure 2.

$$\text{fitness} = (w1 \times \text{fuel cycle length}) + (w2 \times \Delta k_{\infty}) \quad (1)$$

**Table 3** Weight factor variation.

| Variation | Weight Fraction | |
|---|---|---|
| | w1 | w2 |
| A | 0.55 | 4500 |
| B | 0.6 | 4000 |
| C | 0.65 | 3500 |
| D | 0.7 | 3000 |
| E | 0.75 | 2500 |

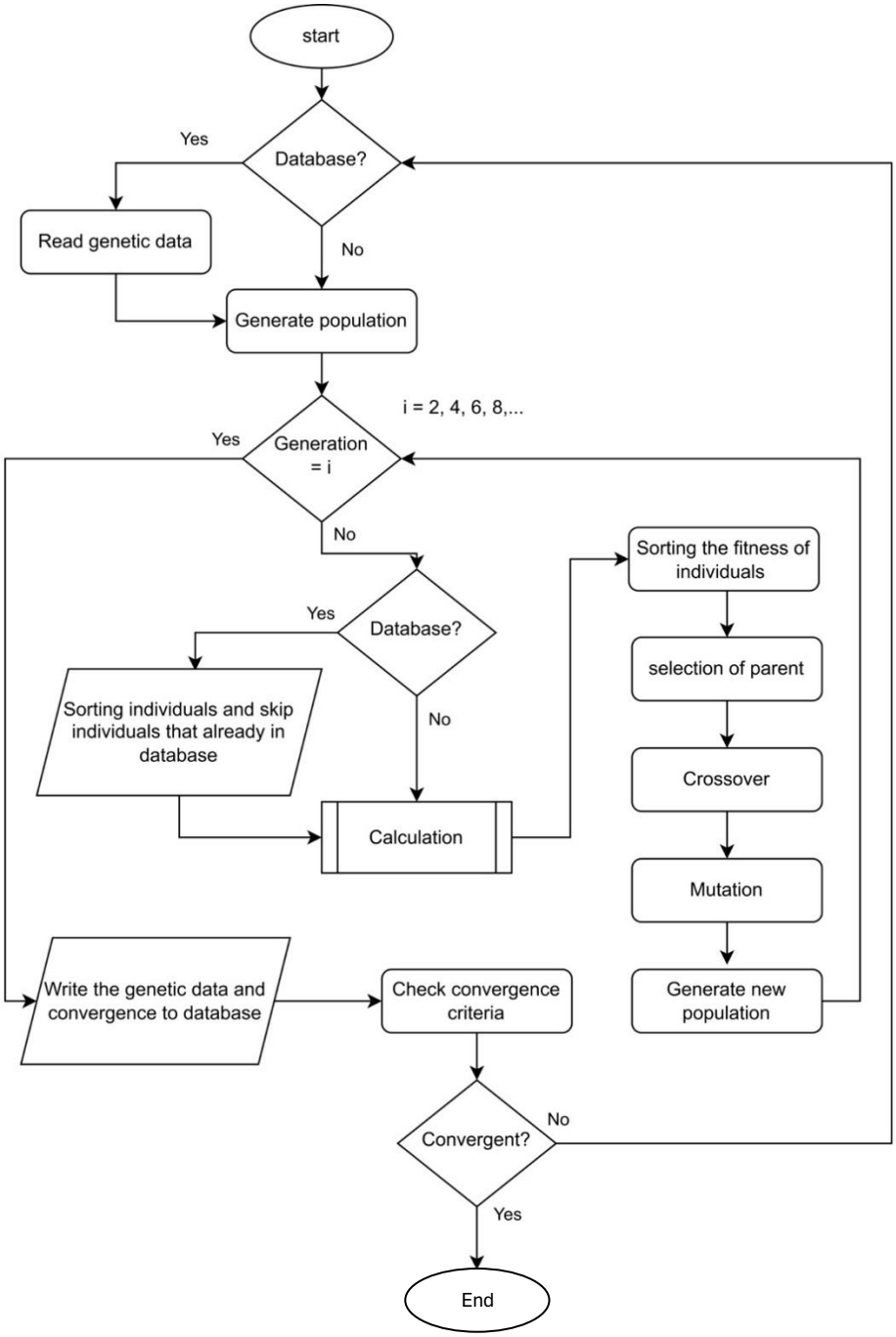


**Figure 2** The flowchart of the Genetic Algorithm.

Several input parameters are needed to dictate the optimization and determine the performance of the algorithm, as listed in Table 4. The number of individuals within the population will affect the initial search space with a smaller number, the search would be limited, and the solution could converge prematurely. A total of 80 individuals are selected as the population to increase the probability of global optima. A value will be assigned to each individual that represents how robust that individual is and this value is called fitness. In addition, a selection is carried out as the component that guides the algorithm to the optimal solution by preferring individuals with high fitness [25]. The mutation rate will also affect the search or the exploration with a higher rate, the algorithm will search for more solutions within the search space. The mutation prevents the algorithm from falling within the local maximum and converging prematurely [26]. Meanwhile, limitations result from the imbalanced nature of exploration and exploitation. The implementation of elitism through iteration balances the exploration and exploitation in the algorithm to solve the problem.

**Table 4** Input parameters in the algorithm.

| Parameter | Value | Unit |
|---|---|---|
| Population | 80 | individual |
| Iteration | 2 | generation |
| Mutation rate | 50% | - |
| Convergence limit | 0.00001 | - |

The mechanism of elitism is not found in the conventional genetic algorithm. This is based on the use of iteration and a database where the parent will be selected as the fittest individuals across generations. In addition, there is no chance for the generation to show an inferior trait.

After obtaining the result from the optimization, further analysis needs to be performed. The analysis examines the assemblies' initial multiplication factor, fuel cycle length, and power peaking factor (PPF). The examination of the parameters occurs at BOC, $k_\infty$ peak, middle-of-cycle (MOC), and EOC. The assembly with the lowest excess reactivity is given a higher rank for the initial multiplication factor. For fuel cycle length, the longest receives a higher rank and the assembly with the lower PPF value is selected in PPF analysis. For each of the solutions, the analysis provides a specific score to represent the rank. Based on the score, the highest-ranked fuel assembly is the best solution. Comparative research on the effect of burnable poison on the basic fuel assembly configuration from the research by FNPP team is performed. This is based on the same research parameters, initial multiplication factor, fuel cycle length, and PPF.

## 3. Results and discussion

### *3.1 Weight factor selection*

The selection of the weight is based on the behavior of the fitness concerning the objectives. The value needs to satisfy the priority with fitness as the sole factor in algorithm selection. The range between the first and second weights is needed to accommodate for the difference in the value of the objective. In addition, the relationship is presented in Figures 3 to 7 for all variations. For the first objective, a lower weight value led to oscillating fitness. Meanwhile, for the second objective, a lower weight value did not affect fitness. In this context, the second objective does not behave differently since the variation of the weight seems to be viable. For the first objective, the difference in weight value affects the fitness significantly and an increase reduces the oscillation of the fitness, with the slightest appearing in variation E. Considering the desired fitness behavior for linearity, the optimal choice for formulating the function in the optimization process is to assign the weight to variation E.

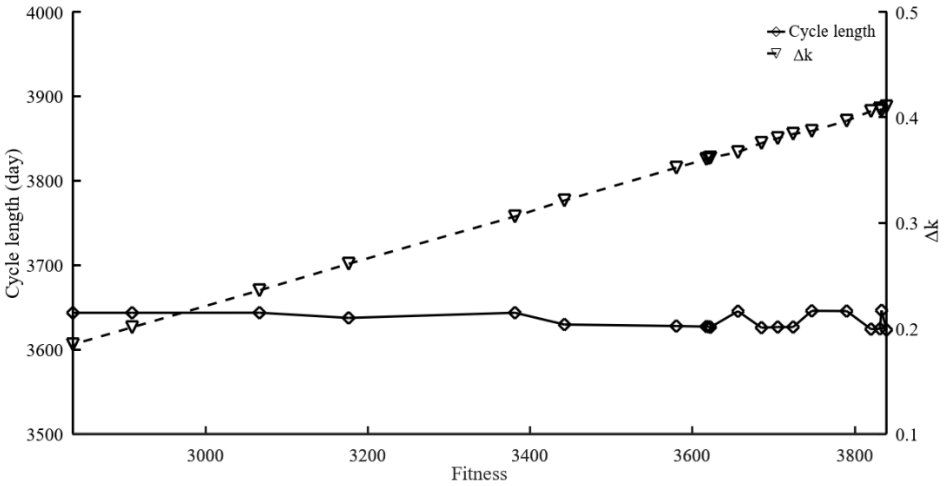


**Figure 3** Relation between objectives and fitness of the variation A.

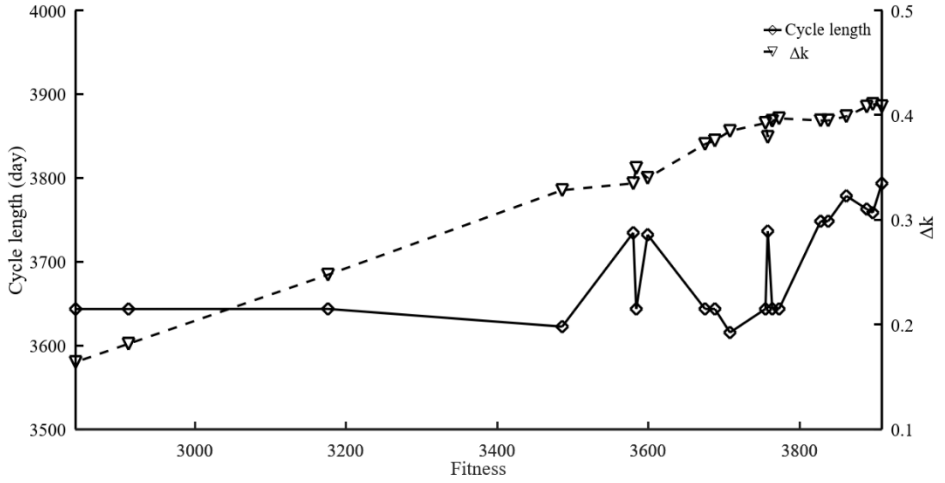


**Figure 4** Relation between objectives and fitness of the variation B.

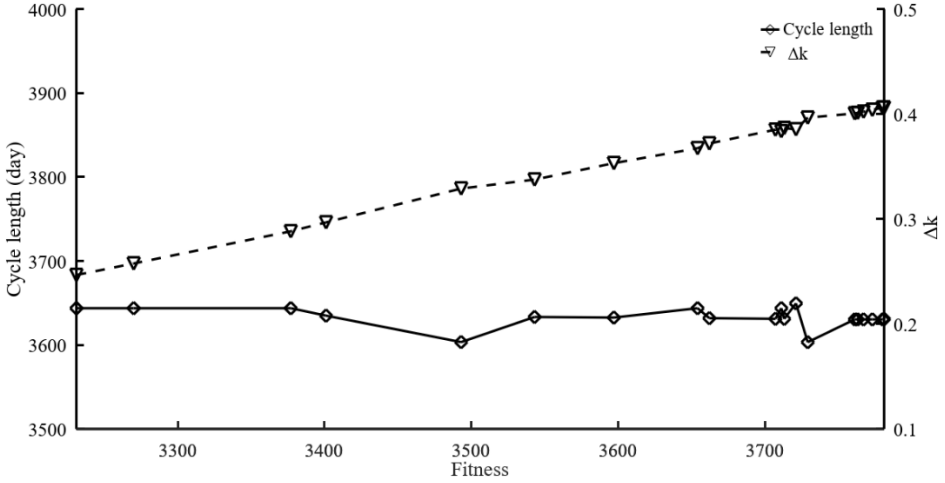


**Figure 5** Relation between objectives and fitness of the variation C.

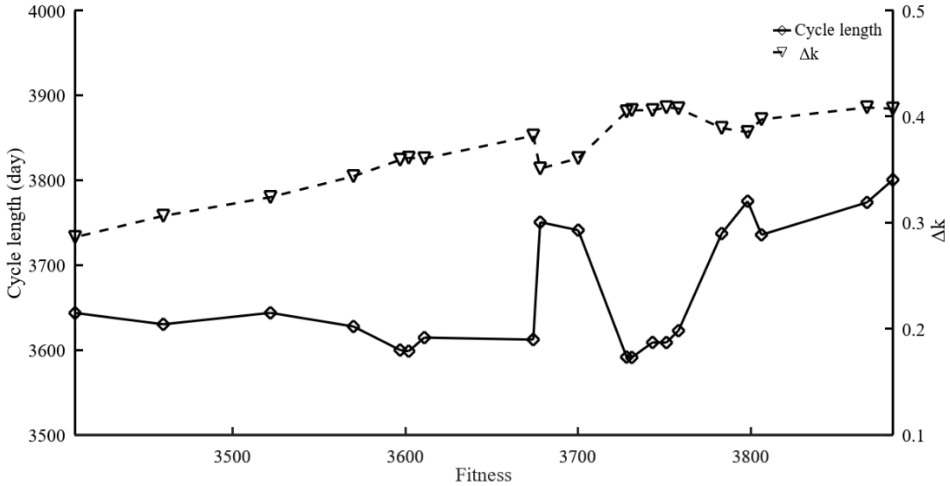


**Figure 6** Relation between objectives and fitness of the variation D.

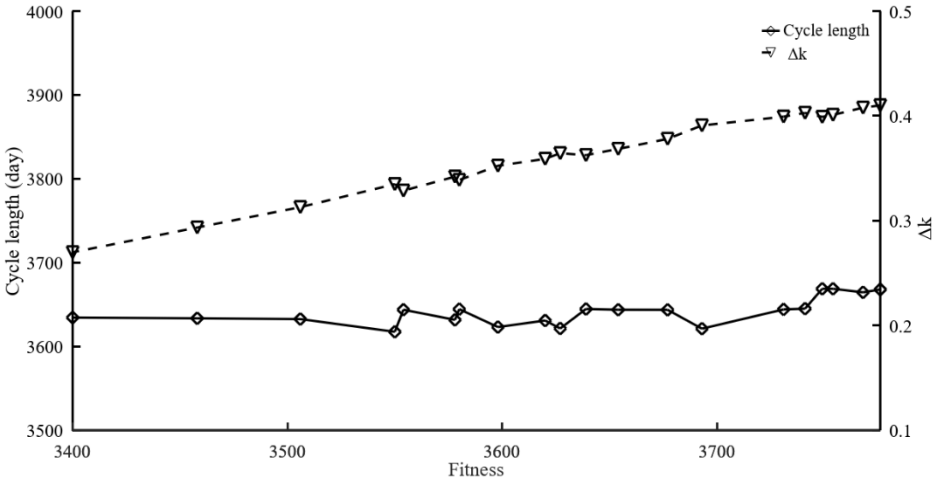


**Figure 7** Relation between objectives and fitness of the variation E.

*3.2 Optimization and comparison from the basic design*

Optimization was carried out simultaneously for eight pin sizes, from 10×10 to 17×17, using Genetic Algorithm. The process followed the algorithm, with the calculation performed by a solver (Polaris). The refinement of the optimization was performed in a cycle consisting of two generations. In each cycle, a process of exploration and exploitation was considered. Elitism is used for continuous exploitation throughout generations while the exploration is only carried out in promising space. The number of cycles needed to determine the optimal solution varies in each pin size. The number of search variables will affect the search and the process can be completed in a few generations for search variables. For more extensive search variables, the search can take up to tens of generations. The criterion for ending the search is based on convergence. In addition, when the difference in fitness within a generation is no greater than $10^{-5}$, the search is stopped, and the optimal solution is obtained.

The result of the optimization process performed for all the pin sizes is shown in Table 5. The result varies for each pin size, with the poison ratio around 0.13% - 2.78%, while seven out of eight poison types resulted in IFBA. The type and placement of the poison pin appear to be influenced by the selection process, hence, the objectives are fulfilled with the configurations.

**Table 5** Result from the optimization for each fuel assembly configuration.

| Pin | Poison ratio (%) | Poison type | Poison placement |
|---|---|---|---|
| 10×10 | 0.66 | IFBA | A 0.013 mm layer of coating |
| 11×11 | 0.3 | IFBA | A 0.006 mm layer of coating |
| 12×12 | 2.78 | IFBA | A 0.051 mm layer of coating |
| 13×13 | 0.14 | IFBA | A 0.003 mm layer of coating |
| 14×14 | 0.35 | IFBA | A 0.009 mm layer of coating |
| 15×15 | 0.13 | Homogenous burnable poison | Mixed within the fuel pellet |
| 16×16 | 0.24 | IFBA | A 0.005 mm layer of coating |
| 17×17 | 0.29 | IFBA | A 0.006 mm layer of coating |

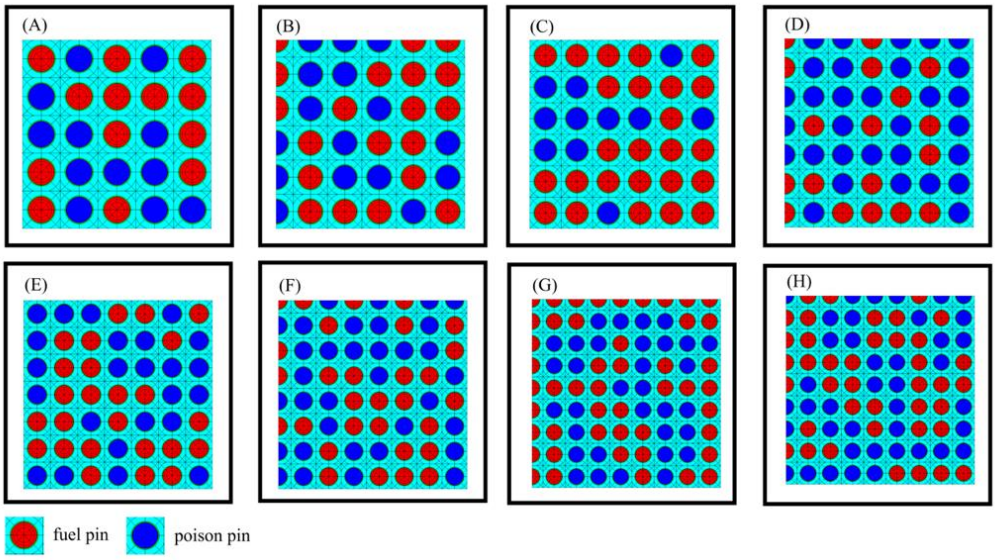


**Figure 8** Poison configuration of the fuel assembly configuration, the map is a quarter southeast symmetry, in which (A) 10×10 pin configuration, (B) 11×11 pin configuration, (C) 12×12 pin configuration, (D) 13×13 pin configuration, (E) 14×14 pin configuration, (F) 15×15 pin configuration, (G) 16×16 pin configuration, and (H) 17×17 pin configuration.

The result from the optimization process will give eight candidates with the poison configuration shown in Figures 8A, 8B, 8C, 8D, 8E, 8F, 8G and 8H, respectively. These individuals are selected based on the initial multiplication factor, fuel cycle length, and PPF, as presented in Table 6. The result shows that the difference in the initial multiplication factor does not vary greatly, ranging from 1.0037 to 1.0141. Meanwhile, the difference for fuel cycle length and PPF range from 3580.44 to 3644.41 and 1.2789 to 1.4522, respectively.

The parameter affects the others substantially reducing the initial multiplication factor by introducing a burnable absorber material will affect the local power generation by dropping the power on the pin with poison. As the total power is kept constant, it increases the neutron flux and the corresponding power generation in other spots, increasing the power peaking factor. Burnable absorber presence on EOC will shorten the cycle due to parasitic absorption, thereby shortening the length. Factors including each assembly's basic configuration (i.e., fuel enrichment, fuel radius, P/D) influence the optimization result. The fuel cycle length is primarily impacted by the inherent capacity of the basic configuration. Therefore, the quantity of fuel remains constant, leading to a marginal increase in the cycle length. The initial multiplication factor and PPF remain unaffected since the two parameters are controlled by the presence of burnable poison.

**Table 6** Result from analysis of each fuel assembly's parameters.

| Fuel assembly (Figure 8) | Initial $k_\infty$ | Fuel cycle length (day) | Time to reach $k_\infty$ peak (day) | BOC PPF | $k_\infty$ peak PPF | MOC PPF | EOC PPF | Maximum PPF |
|---|---|---|---|---|---|---|---|---|
| A | 1.0054 | 3644.41 | 450 | 1.2789 | 1.0114 | 1.0037 | 1.0037 | 1.2789 |
| B | 1.0082 | 3626.23 | 240 | 1.4064 | 1.0048 | 1.0019 | 1.0018 | 1.4064 |
| C | 1.0141 | 3637.43 | 720 | 1.4421 | 1.0104 | 1.0094 | 1.0094 | 1.4421 |
| D | 1.0037 | 3623.23 | 180 | 1.3431 | 1.0039 | 1.0014 | 1.0013 | 1.3431 |
| E | 1.0078 | 3638.14 | 240 | 1.3263 | 1.0081 | 1.0018 | 1.0018 | 1.3263 |
| F | 1.0066 | 3603.77 | 180 | 1.4522 | 1.0030 | 1.0022 | 1.0016 | 1.4522 |
| G | 1.0071 | 3617.22 | 180 | 1.4112 | 1.0083 | 1.0024 | 1.0024 | 1.4112 |
| H | 1.0062 | 3580.44 | 240 | 1.3500 | 1.0063 | 1.0018 | 1.0017 | 1.3500 |

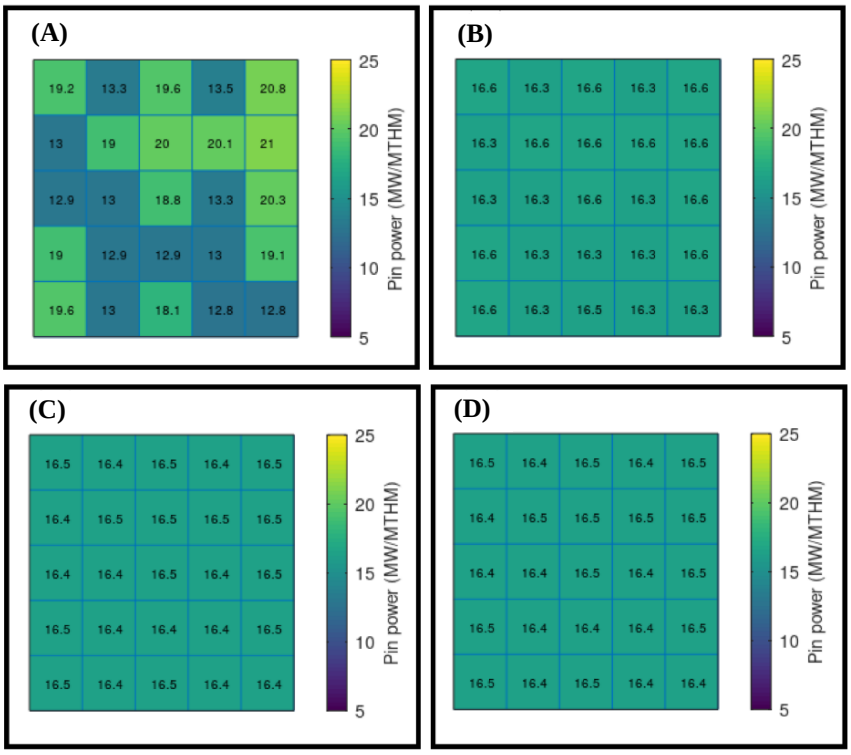


**Figure 9** The pin power distribution of 10×10 configuration with poison, in which (A) at BOC, (B) at $k_\infty$ peak, (C) at MOC, and (D) at EOC.

All configurations with poison follow the same behavior, where the highest PPF is observed at BOC and decreases substantially towards EOC, as shown in Figures 9A, 9B, 9C and 9D. The presence of burnable poison significantly influences the behavior and at BOC, the concentration is highest, resulting in increased PPF. Towards $k_\infty$ peak, PPF decreased substantially, marking a significant reduction in burnable poison. In MOC and EOC, PPF is lower, with some configurations showing the same result. There is a subtle difference in PPF value of others between MOC and EOC. The discernible variations during the phase of the fuel cycle in some configurations can be attributed to the phenomenon of parasitic absorption. This observation serves as evidence that burnable poison is still present in the fuel.

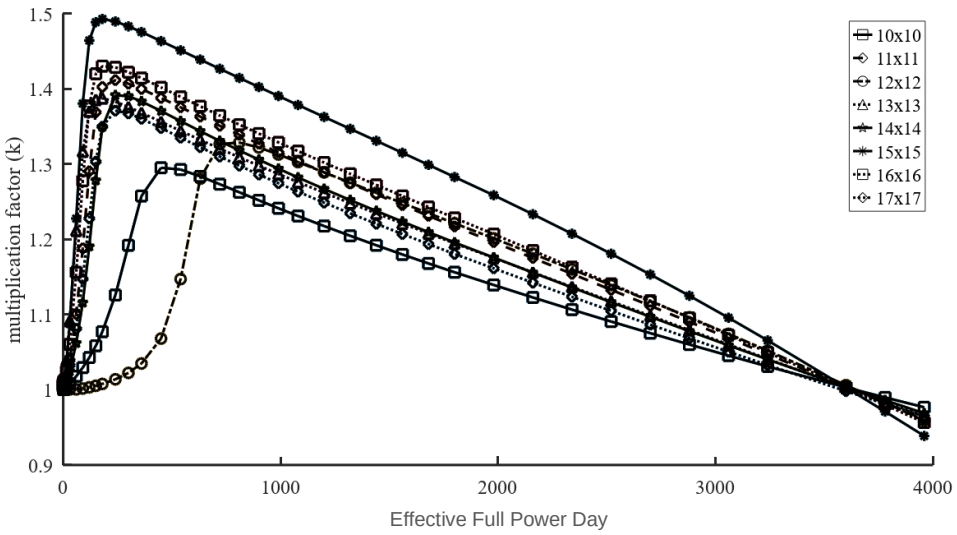


**Figure 10** Burnup of each fuel assembly configuration.

**Table 7** Comparison of the basic and new design parameters.

| Pin | | Initial multiplication factor | Fuel cycle length (day) | Maximum PPF |
|---|---|---|---|---|
| 10×10 | Basic | 1.4107 | 3645.82 | 1.0005 |
| | New | 1.0054 | 3644.41 | 1.2789 |
| 11×11 | Basic | 1.4898 | 3623.28 | 1.0009 |
| | New | 1.0082 | 3626.23 | 1.4064 |
| 12×12 | Basic | 1.4694 | 3619.91 | 1.0005 |
| | New | 1.0141 | 3637.43 | 1.4421 |
| 13×13 | Basic | 1.4521 | 3621.62 | 1.0006 |
| | New | 1.0037 | 3623.23 | 1.3431 |
| 14×14 | Basic | 1.4834 | 3635.81 | 1.0001 |
| | New | 1.0078 | 3638.14 | 1.3263 |
| 15×15 | Basic | 1.5688 | 3603.08 | 1.0002 |
| | New | 1.0066 | 3603.77 | 1.4522 |
| 16×16 | Basic | 1.5051 | 3614.75 | 1.0015 |
| | New | 1.0071 | 3617.22 | 1.4112 |
| 17×17 | Basic | 1.4548 | 3632.75 | 1.0012 |
| | New | 1.0062 | 3580.44 | 1.3500 |

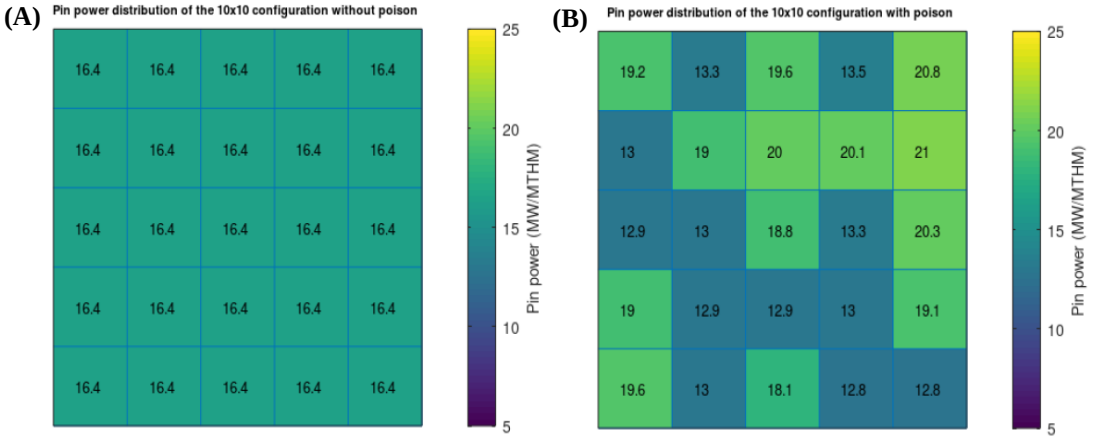


**Figure 11** The comparison in pin power distribution of 10×10 configuration without (A) and with poison introduction (B).

A comparison analysis for the basic and new configurations has been conducted. Table 7 shows the result of the parameters for all configurations. The use of burnable poison produces a recurring circumstance in the configurations. A decrease in the initial multiplication factor occurs considering the use of burnable poison. Meanwhile, most of the fuel cycle length is increased slightly, except for the configuration of 10×10 and 17×17. The increase shows that the poison is consumed thoroughly toward EOC, leading to the absence of parasitic absorption. In this context, 70% enriched Gd lowers parasitic absorption, as reported by Bejmer and Steveborn [16]. As for PPF, an increase is observed in all the configurations. The anticipated rise is a natural outcome since the presence of burnable poison undeniably influences neutron behavior in the immediate vicinity. This effect leads to a reduction in power generation on the pins containing the poison, while simultaneously elevating others. Figures 11A and 11B show the difference in pin power distribution of the 10×10 configuration. By introducing burnable poison, a substantial increase in PPF is observed at BOC. In the case of 10×10 configuration, the increase is from 1.0005 to 1.2789. Even though this can be considered a limitation, PPF will return to the original values as burnable poison depletes.

### *3.3 Selection of the Final Solution*

Table 8 shows the score of each configuration before conducting the final selection. Pin 10×10 configuration appears to be the highest-ranked configuration, with a score of 29. In addition, the configuration has the most extended fuel cycle, lowest PPF, and second lowest initial multiplication factor. This configuration's initial $k_\infty$ and cycle length are 1.0054 and 3644.41, respectively.

**Table 8** The score of parameters for each design.

| Pin | Initial multiplication factor score | Fuel cycle length score | PPF score | Total score |
|---|---|---|---|---|
| 10×10 | 9 | 10 | 10 | 29 |
| 11×11 | 4 | 7 | 6 | 17 |
| 12×12 | 3 | 8 | 3 | 14 |
| 13×13 | 10 | 6 | 8 | 24 |
| 14×14 | 5 | 9 | 9 | 23 |
| 15×15 | 7 | 4 | 4 | 15 |
| 16×16 | 6 | 5 | 5 | 16 |
| 17×17 | 8 | 3 | 7 | 18 |

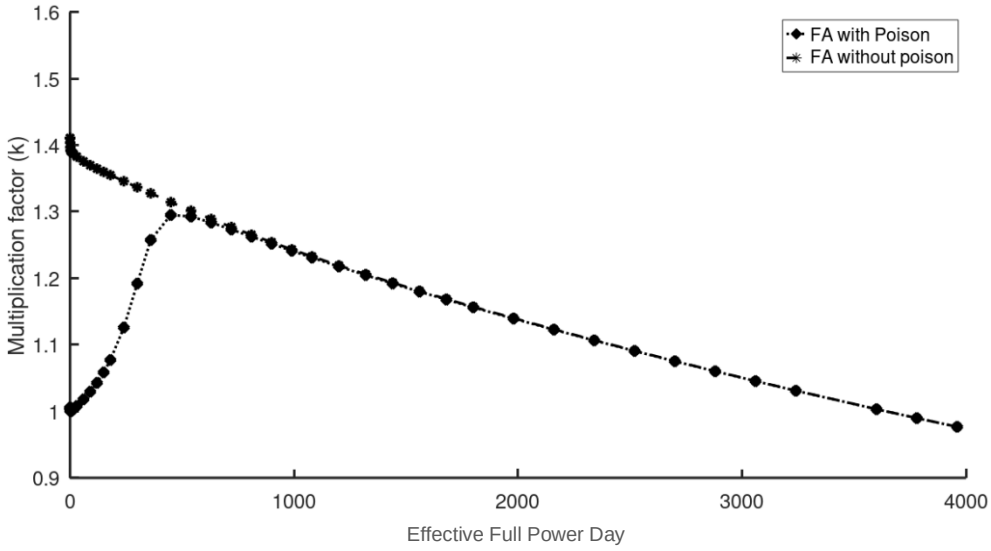


**Figure 12** The effect of burnable poison in the fuel assembly on the evolution of multiplication factor.

The initial multiplication factor has been reduced from 1.4107 to 1.0054, as shown in Figure 11 and the problem regarding excess reactivity has been solved. The reduced excess reactivity allowed for a straightforward control system, which led to an advantage for operation in remote regions. Meanwhile, the addition of burnable poison in the fuel assembly has lowered multiplication factor without compromising the cycle length. Figure 12 shows that Gd has been consumed almost entirely at 540 days, with the residual amount present until around 900 days.

The fuel cycle length has been maintained close to 10 years, allowing an extended operational time for the reactor without additional supply or resources. The maximum PPF of 1.2789 is considered acceptable and falls within the typical range of most PWRs between 1.2 and 1.3. Based on the final selection, the fuel assembly configuration is presented in Table 9. This follows the basic configuration with the addition of a 0.0013 mm coating of burnable poison in the selected pins.

**Table 9** The fuel assembly configuration from the final selection.

| Configuration of the selected fuel assembly | |
|---|---|
| Pin | 10×10 |
| Fuel material | $U_3Si_2$ |
| Cladding material | FeCrAl |
| P/D | 1.34 |
| Fuel radius (m) | 0.004033 |
| Cladding thickness (m) | 0.0003 |
| Total diameter (m) | 0.008846 |
| Fuel enrichment (%) | 7.7 |
| Poison ratio (%) | 0.66 |
| Poison type | IFBA |
| Fuel radius (m) in poison pin | 0.00402 |
| Poison placement in pin | A 0.013 mm layer of coating |
| Poison configuration | Figure 8 (A) |

## 4. Conclusion

In conclusion, the optimization process was conducted successfully and the design satisfied the objectives. The final design was a 10×10 configuration with a 0.66% poison ratio and 48 IFBA pins. Additionally, the initial multiplication factor was reduced from 1.4107 to 1.0054, and the fuel cycle decreased slightly from 3645.82 days to 3644.41 days. The maximum PPF of 1.2789 was observed at BOC. The use of more objectives regarding performance parameters was recommended for future optimization research. Other parameters, such as PPF and feedback reactivity temperature coefficient ensure the solution does not violate any standards. Meanwhile, a subsequent core design and analysis should be performed with consideration of the results. The maximum excess reactivity issue after the introduction of burnable poison must also be addressed in future research.

## 5. References


[1] Mulyana R. Performance report of the general secretary of energy and mineral resources 2022. Jakarta: Indonesian Ministry of Energy and Mineral Resources; 2022.

[2] Advanced reactor information system (ARIS). Small modular reactor technology catalogue 2024. Vienna: International Atomic Energy Agency; 2024.

[3] Agung A, Sihana, Suryopratomo K. Final report on the development of floating nuclear power plant to fulfill energy requirements in remote areas. Yogyakarta: Universitas Gadjah Mada; 2022.

[4] Torabi M, Lashkari A, Masoudi SF, Bagheri S. Neutronic analysis of control rod effect on safety parameters in Tehran Research Reactor. Nucl Eng Technol. 2018;50:1017–1023.

[5] Nerlander V. Power increase limits to prevent pellet-cladding interaction: Calculation of strain- and fission gas release margins [dissertation]. Uppsala: Uppsala University; 2022.

[6] Human resources training and development. GE BWR/4 advanced technology manual. Chapter 4.4: Pre-conditioning interim operating management guidelines. Washington, DC: United States Nuclear Regulatory Commission; 2004.

[7] Papukchiev A, Liu Y, Schaefer A. Impact of boron dilution accidents on low boron PWR safety. Proceedings of the physics of fuel cycles and advanced nuclear systems: Global developments; 2006 September 10-14; Vancouver, Canada, American Nuclear Society; 2006.

[8] Evans JA, DeHart MD, Weaver KD, Keiser DD. Burnable absorbers in nuclear reactors – A review. Nucl Eng Des. 2022;391:111726.

[9] J A Renier. Development of improved burnable poisons for commercial nuclear power reactors. Technical Report. Oak Ridge, TN (United States): Oak Ridge National Lab (ORNL); 2002 Apr. Report No.: ORNL/TM-2001/238.

[10] van der Merwe L, Hah CJ. Reactivity balance for a soluble boron-free small modular reactor Nucl Eng Technol. 2018;50:648–653.

[11] Mart J, Klein A, Soldatov A. Feasibility study of a soluble boron–free small modular integral pressurized water reactor. Nucl Technol. 2014;188(1):8–19.

[12] Marguet S., editor The technology of pressurized water reactors: From the nautilus to the EPR. Vol. 1. Cham, Switzerland: Springer International Publishing; 2022.

[13] Jo CK, Kim Y, Noh JM. Burnable poison for reactivity management in a very high temperature reactor. Ann Nucl Energy. 2009;36(3):298–304.

[14] Dodd B, Britt T, Lloyd C, Shah M, Goddard B. Novel homogeneous burnable poisons in pressurized water reactor ceramic fuel. Nucl Eng Technol. 2020;52(12):2874–2879.

[15] Xu S, Yu T, Xie J, Yao L, Li Z. Burnable poison selection and neutronics analysis of plate fuel assemblies. Front Energy Res 2021;9:729552.

[16] Bejmer KH, Seveborn O. Enriched Gadolinium as burnable absorber for PWR. Proceedings of the physics of fuel cycles and advanced nuclear systems: Global developments; 2004 April 25-29; La Grange Park, Chicago, USA, American Nuclear Society; 2004. p. 1245-1253.

[17] Jayalal ML, Sai Baba M, SatyaMurty SAV. Application of Genetic Algorithm for optimization of fuel management in nuclear reactors. 2016 International Conference on Data Mining and Advanced Computing (SAPIENCE), Ernakulam, India: IEEE; 2016. p. 325–330.

[18] Yilmaz S, Ivanov K, Levine S, Mahgerefteh M. Application of genetic algorithms to optimize burnable poison placement in pressurized water reactors. Ann Nucl Energy. 2006;33(5):446–456.

[19] Jessee MA, Wieselquist WA, Mertyurek U, Kim KS, Evans TM, Hamilton SP, et al. Lattice physics calculations using the embedded self-shielding method in Polaris, Part I: Methods and implementation. Ann Nucl Energy. 2021;150:107830.

[20] Chen Q, Wu H, Cao L. Auto MOC-A 2D neutron transport code for arbitrary geometry based on the method of characteristics and customization of AutoCAD. Nucl Eng Des. 2008;238(10):2828–2833.

[21] Cao L, Wu H, editors. Deterministic numerical methods for unstructured-mesh neutron transport calculation. Woodhead Publishing; 2020.
[22] Isotalo A, Pusa M. Improving the accuracy of the Chebyshev rational approximation method using substeps. Nucl Sci Eng. 2016;183(1):65–77.
[23] Calvin O, Schunert S, Ganapol B. Global error analysis of the Chebyshev rational approximation method. Ann Nucl Energy. 2021;150:107828.
[24] Stewart RH, Palmer TS, DuPont B. A survey of multi-objective optimization methods and their applications for nuclear scientists and engineers. Prog Nucl Energy. 2021;138:103830.
[25] Nayak S. Nature-inspired optimization. In: Nayak S, editor. Fundamentals of optimization techniques with algorithms, Elsevier; 2020. p. 271–296.
[26] Arthur J, Bahran R, Hutchinson J, Pozzi SA. Genetic algorithm for nuclear data evaluation applied to subcritical neutron multiplication inference benchmark experiments. Ann Nucl Energy. 2019;133:853–862.